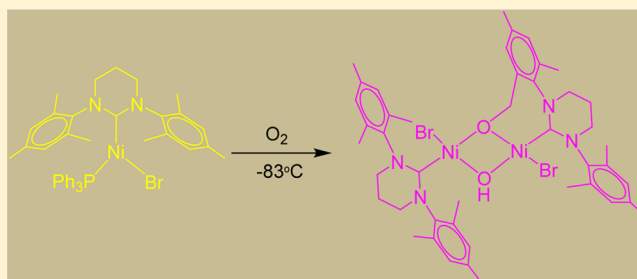


Stereochemical Effects in C–H Bond Oxidation Reactions of Ni(I) N-Heterocyclic Carbene Complexes

Rebecca C. Poulten,[†] Isidoro López,[‡] Antoni Llobet,[‡] Mary F. Mahon,[†] and Michael K. Whittlesey^{*,†}[†]Department of Chemistry, University of Bath, Claverton Down, Bath BA2 7AY, U.K.[‡]Institute of Chemical Research of Catalonia (ICIQ), Avinguda Paisos Catalans 16, E-43007 Tarragona, Spain

Supporting Information

ABSTRACT: Activation of O₂ by the three-coordinate Ni(I) ring-expanded N-heterocyclic carbene complexes Ni(RE-NHC)(PPh₃)Br (RE-NHC = 6-Mes, **1**; 7-Mes, **2**) produced the structurally characterized dimeric Ni(II) complexes Ni(6-Mes)(Br)(μ-OH)(μ-O-6-Mes')NiBr (**3**) and Ni(7-Mes)(Br)(μ-OH)(μ-O-7-Mes')NiBr (**4**) containing oxidized *ortho*-mesityl groups from one of the carbene ligands. NMR and mass spectrometry provided evidence for further oxidation in solution to afford bis-μ-aryloxy compounds; the 6-Mes derivative was isolated, and its structure was verified. Low-temperature UV–visible spectroscopy showed that the reaction between **1** and O₂ was too fast even at ca. –80 °C to yield any observable intermediates and also supported the formation of more than one oxidation product. Addition of O₂ to Ni(I) precursors containing a less electron-donating diamidocarbene (6-MesDAC, **7**) or less bulky 6- or 7-membered ring diaminocarbene ligands (6- or 7-*o*-Tol; **8** and **9**) proceeded quite differently, affording phosphine and carbene oxidation products (Ni(O=PPh₃)₂Br₂ and (6-MesDAC)=O) and the mononuclear Ni(II) dibromide complexes (Ni(6-*o*-Tol)(PPh₃)Br₂ (**10**) and (Ni(7-*o*-Tol)(PPh₃)Br₂ (**11**)) respectively. Electrochemical measurements on the five Ni(I) precursors show significantly higher redox potentials for **1** and **2**, the complexes that undergo oxygen atom transfer from O₂.



INTRODUCTION

In contrast to the well-known ability of Ni(0) to coordinate and activate small gaseous molecules,¹ a comparable appreciation of the reactivity of Ni(I) is very much still in its infancy, predominantly because there are relatively few isolated and fully characterized Ni(I) complexes.² Small molecule coordination/activation at monovalent nickel is therefore first and foremost of considerable fundamental interest,^{3,4} but also of practical importance because Ni(I) is known to be central to a number of enzymatic processes.⁵ In methyl-coenzyme M reductase (MCR), for example, the nickel(I) cofactor F430 (Scheme 1a) catalyzes the reduction of methyl-coenzyme M (methyl-SCoM) by coenzyme B (CoB-SH) to give CH₄ and the heterodisulfide CoB–S–S–CoM.⁶ In terms of mechanism, isotopic labeling experiments have suggested that a Ni(I) σ-CH₄ intermediate may lie on the reaction pathway.⁷ In CO dehydrogenase/acetyl coenzyme A synthase, a three-coordinate monovalent Ni center (the so-called Ni_p site; Scheme 1b) coordinates CO before undergoing methylation and migratory insertion to afford the final acetyl group.⁸

In order to develop a correlation between the structures of Ni(I) complexes and their reactivity toward small molecules, new examples of Ni(I) species are required. Ideally, such species would be based upon easily modifiable ligand sets, since this would allow the stereochemical properties of the metal center to be readily altered in a very controllable way. In this

respect, we have recently reported the preparation and characterization of a series of three-coordinate Ni(I) complexes of the type Ni(RE-NHC)(PPh₃)X (X = Br, Cl) containing ring-expanded N-heterocyclic carbene (RE-NHC) ligands based on N-aryl substituted six-, seven-, and eight-membered rings (Chart 1).⁹ Using a combination of continuous wave and pulsed EPR measurements in conjunction with DFT calculations, we showed that the spin Hamiltonian parameters in these d⁹ systems were sensitive to variations in both ring size and N-substituent and, furthermore, that the admixture of |3d_{z²}⟩ and |3d_{x²-y²}⟩ character that made up the SOMO varied from one complex to another.

Given the variations in electronic structure therefore apparent in this range of compounds, we have now moved our focus to consider their reactivities. In many of our early efforts to prepare the 6-Mes derivative **1**, we observed that inadvertent exposure of yellow, highly air-sensitive solutions of **1** to even trace amounts of oxygen resulted in an extremely rapid color change to purple. We now report that this color change is associated with the activation of O₂ by **1** and the formation of a dimeric Ni(II) complex **3** containing a 6-Mes ligand oxidized at one of the *ortho*-methyl C–H groups. Both **1** and the corresponding 7-Mes complex **2**, which reacts similarly,

Received: January 28, 2014

Published: June 27, 2014

Scheme 1

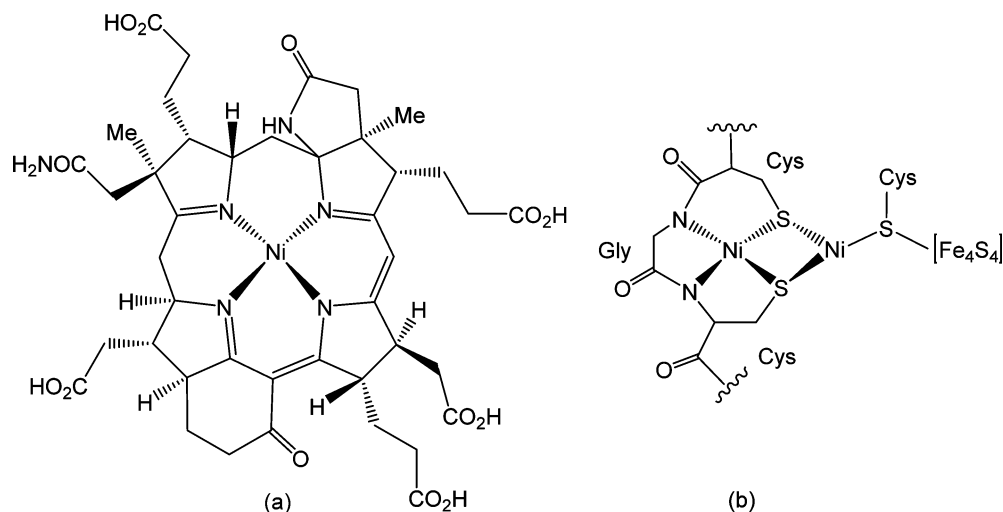
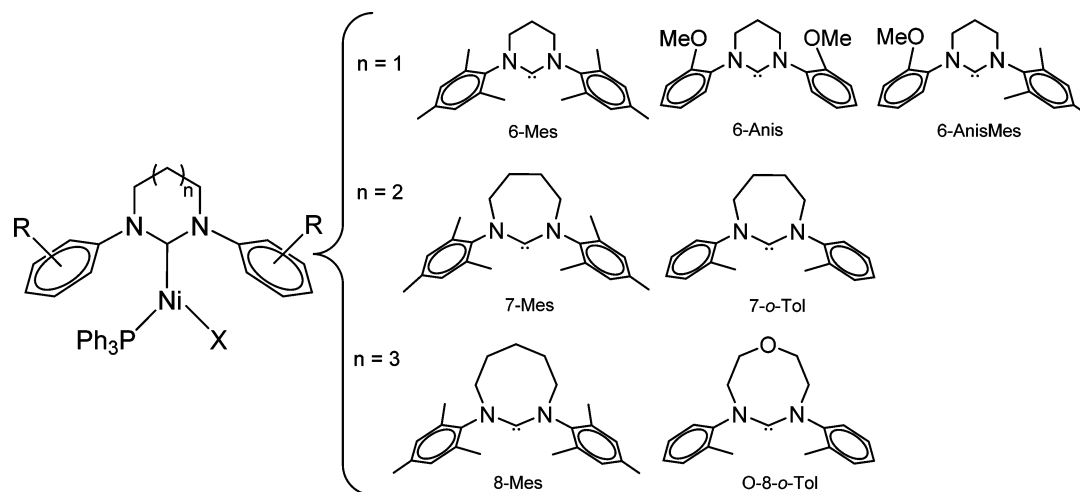


Chart 1



also undergo further reaction to afford the doubly oxidized products $\text{Ni}(\text{Br})(\mu\text{-O-6-/7-Mes}')_2\text{NiBr}$. In contrast, Ni(I) precursors bearing either a less electron-rich diamidocarbene (DAC) or a less bulky *N-ortho*-tolyl substituted diaminocarbene exhibit quite different reactivity toward O_2 , generating mononuclear Ni(II) species that result from phosphine oxidation or halide redistribution reactions rather than oxidation of the NHC ligand.¹⁰

EXPERIMENTAL SECTION

All manipulations were carried out using standard Schlenk, high vacuum, and glovebox techniques using dried and degassed solvents. NMR spectra were recorded in C_6D_6 (referenced to δ 7.15 and 128.0), CD_2Cl_2 (δ 5.32 and 54.5), and CDCl_3 (δ 7.24) on Bruker Avance 400 and 500 MHz NMR spectrometers. ^{31}P NMR spectra were referenced to 85% H_3PO_4 at δ 0.0. Mass spectra were recorded on a Bruker MicrOTOF electrospray time-of flight (ESI-TOF) mass spectrometer (Bruker Daltonik GmbH) coupled to an Agilent 1200 LC system (Agilent Technologies). Elemental analyses were performed by the Elemental Analysis Service, London Metropolitan University, London, U.K.

CV experiments were carried out in an MBraun glovebox ($\text{O}_2 < 0.1$ ppm, $\text{H}_2\text{O} = 0.3$ ppm) using a IJ-Cambria CHI-660 potentiostat with anhydrous inhibitor-free THF (containing 0.1 M $[\text{tBu}_4\text{N}]\text{PF}_6$) as solvent. Glassy carbon disks were used as the working electrode, Pt

wire as a counter electrode, and Ag wire as a quasi-reference electrode. The CVs were run at 100 mV s^{-1} scan rate and the potentials were referenced to ferrocene (added at the end of each experiment) and subsequently converted to NHE. UV–visible spectroscopy was performed on a CARY 50 (Varian) UV–visible spectrophotometer using an all-quartz immersion probe with 1 cm optical path length from Hellma. The temperature was kept constant at -83°C by means of a liquid N_2 /acetone bath and monitored by a low-temperature thermometer. Kinetic data were processed by use of the program SPECFIT/32 Global Analysis System, which uses the method of singular value decomposition (SVD).

Complexes **1**, **2**, **9**, and 6-MesDAC, were prepared according to the literature.^{9,11} $\text{Ni}(\text{cod})_2$ and $\text{Ni}(\text{PPh}_3)_2\text{Br}_2$ were purchased from Sigma-Aldrich.

Reaction of Ni(6-Mes)(PPh₃)Br (1) with O₂. A THF (15 mL) solution of Ni(6-Mes)(PPh₃)Br (140 mg, 0.194 mmol) in an ampule fitted with a J. Youngs resealable PTFE valve was freeze–pump–thaw degassed three times, and the yellow solution was exposed to 1 atm of O_2 , leading to the instantaneous formation of a purple colored solution. After stirring for 5 min, the solvent was removed under vacuum, the residue washed with hexane (10 mL) and then dissolved in $\text{C}_6\text{H}_5\text{F}$ (10 mL). Hexane (20 mL) was added with vigorous stirring to yield **3** as a purple microcrystalline solid. Yield: 47.5 mg (52%). Crystals appropriate for X-ray crystallography were grown from THF/hexane. Anal. calcd (found) for $\text{C}_{44}\text{H}_{56}\text{N}_4\text{O}_2\text{Br}_2\text{Ni}_2$ (%): C 55.62 (55.39), H 5.94 (5.94), N 5.90 (5.85).

Table 1. Crystal Data and Structure Refinement Details for Compounds 3, 4, 5, 7, 10, and 11

	3	4	5	7	10	11
formula	C ₄₄ H ₅₆ Br ₂ N ₄ Ni ₂ O ₂	C ₄₆ H ₆₀ Br ₂ N ₄ Ni ₂ O ₂	C ₄₄ H ₅₄ Br _{0.40} Cl _{1.60} N ₄ Ni ₂ O ₂	C ₄₂ H ₄₃ BrN ₂ NiO ₂ P	C ₃₆ H ₃₃ Br ₂ N ₂ NiP	C ₃₇ H ₃₇ Br ₂ N ₂ NiP
formula mass	950.17	978.22	877.02	777.37	745.16	759.19
cryst syst	monoclinic	triclinic	triclinic	monoclinic	monoclinic	monoclinic
space group	P2 ₁ /n	P $\bar{1}$	P $\bar{1}$	P2 ₁ /n	P2 ₁ /n	P2 ₁ /c
a, Å	14.0430(2)	12.6730(2)	12.8530(2)	11.3530(1)	14.8730(4)	18.4030(1)
b, Å	15.6560(2)	12.8470(3)	13.4070(2)	17.9990(2)	13.5120(4)	9.3870(1)
c, Å	19.5740(3)	16.0810(3)	14.8420(3)	18.3910(2)	17.3700(5)	21.3520(2)
α , deg	90.00	101.027(1)	107.486(1)	90.00	90.00	90.00
β , deg	90.194(1)	110.711(1)	99.498(1)	100.635(1)	109.392(2)	115.468(1)
γ , deg	90.00	104.940(1)	114.349(1)	90.00	90.00	90.00
vol, Å ³	4303.46(11)	2247.65(8)	2095.99(6)	3693.51(7)	3292.71(16)	3330.10(5)
Z	4	2	2	4	4	4
reflms measured	75160	44832	34804	72526	55969	55969
indep reflms	9813	10169	9558	8447	7522	7522
R _{int}	0.0883	0.0605	0.0488	0.0516	0.0760	0.0760
final R _i (I > 2 σ (I))	0.0431	0.0508	0.0370	0.0309	0.0578	0.0578
final wR(F ²) (I > 2 σ (I))	0.0848	0.1226	0.0858	0.0771	0.1399	0.1399
final R _i (all data)	0.0725	0.0809	0.0542	0.0404	0.0941	0.0941
final wR(F ²) (all data)	0.0971	0.1369	0.0935	0.0829	0.1542	0.1542
GOF on F ²	1.100	1.070	1.035	1.047	1.178	1.016

Reaction of Ni(7-Mes)(PPh₃)Br (2) with O₂. Reaction was performed as described in the preceding section but with Ni(7-Mes)(PPh₃)Br (162 mg, 0.220 mmol). Yield of 4: 56.5 mg (52%). X-ray quality crystals were grown from CH₂Cl₂/hexane. Anal. calcd (found) for C₄₆H₆₀N₄O₂Br₂Ni₂ (%): C 55.62 (56.29), H 5.94 (5.97), N 5.90 (5.87).

Ni(6-MesDAC)(PPh₃)Br (7). A THF (20 mL) solution of free 6-MesDAC (386 mg, 1.02 mmol) was added to a mixture of Ni(cod)₂ (139 mg, 0.50 mmol) and Ni(PPh₃)₂Br₂ (381 mg, 0.51 mmol). The mixture was stirred at room temperature for 2.5 h to afford a dark orange solution. After filtration, the filtrate was concentrated, and hexane (20 mL) was added to precipitate a dark purple solid, which was filtered, washed with hexane (10 mL), and dried in vacuo. Yield: 490 mg (62%). X-ray quality crystals were obtained by recrystallization from C₆H₆/hexane. Anal. calcd (found) for C₄₂H₄₃N₂O₂PBrNi (%): C 64.89 (64.61), H 5.58 (5.39), N 3.60 (3.41).

Reactivity of 7 with O₂. A THF (10 mL) solution of Ni(6-MesDAC)(PPh₃)Br (97 mg, 0.125 mmol) was freeze-pump-thaw degassed (3 cycles) and the solution opened to 1 atm O₂. A color change from dark orange-red to nearly colorless ensued in <1 min. After stirring for 5 min, the solution was reduced to dryness, and the residue was washed with hexane (10 mL) to afford a creamy-green material. Recrystallization from CH₂Cl₂/hexane generated 70 mg of a mixture of Ni(O=PPh₃)₂Br₂ and (6-MesDAC)=O. ¹H NMR (400 MHz, CD₂Cl₂, 25 °C): δ 7.82 (br s), 7.03 (br s), 6.72* (s, 4H), 2.07* (s, 12H), 2.05* (s, 6H), 1.61* (s, 6H). The resonances marked with * match with those reported for (6-MesDAC)=O.¹²

Ni(6-o-Tol)(PPh₃)Br (8). [6-o-Tol]BF₄ (153 mg, 0.58 mmol) and K[N(SiMe₃)₂] (116 mg, 0.58 mmol) were dissolved in THF (15 mL) and left stirring for 30 min. After cannula transfer to a mixture of Ni(cod)₂ (80 mg, 0.29 mmol) and Ni(PPh₃)₂Br₂ (215 mg, 0.29 mmol), the solution was left stirring at room temperature for 2 h to afford a dark yellow solution. Cannula filtration and addition of hexane (20 mL) gave a yellow precipitate, which was filtered, washed with hexane (10 mL), and dried under vacuum. Analytically pure product was achieved upon recrystallization from C₆H₆/hexane. Yield: 220 mg (57%). Anal. calcd (found) for C₃₆H₃₅BrN₂NiP (%): C 65.00 (64.81), H 5.30 (5.21), N 4.21 (4.35).

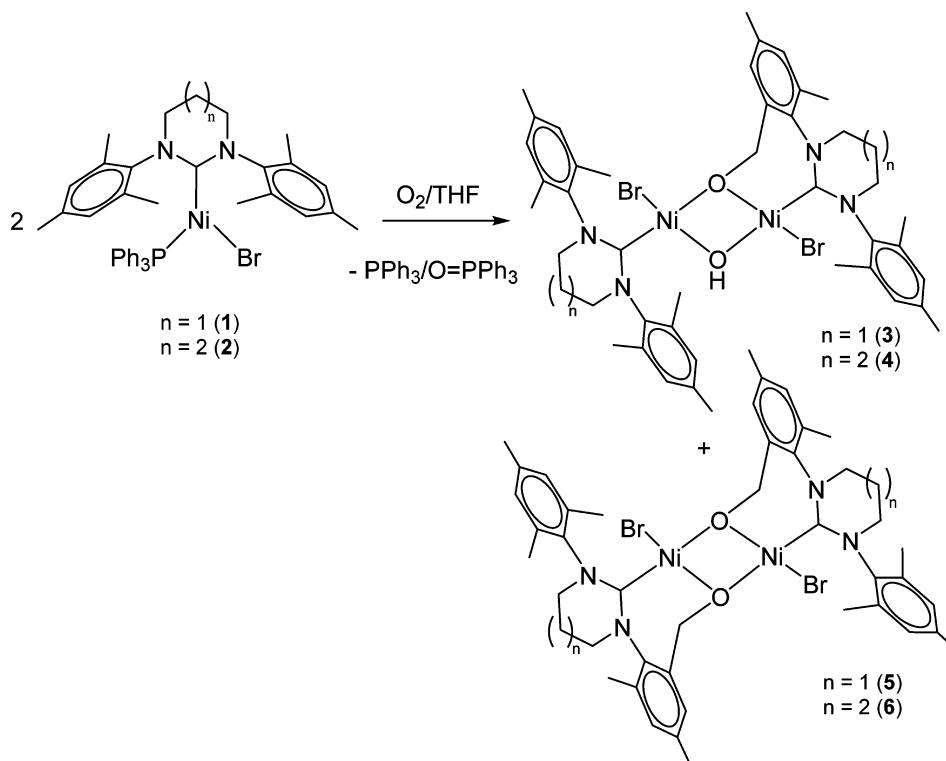
Ni(6-o-Tol)(PPh₃)Br₂ (10). Exposure of a freeze-pump-thaw degassed (three cycles) THF solution (10 mL) of Ni(6-o-Tol)(PPh₃)Br (41 mg, 0.062 mmol) to 1 atm of O₂ led to an instantaneous color change from yellow to purple/red. Removal of the solvent in vacuo

gave a purple/red residue, which was washed with hexane (10 mL), dissolved in C₆H₅F (10 mL), and layered with hexane (20 mL) to give 10 as a purple microcrystalline solid. Yield: 9 mg (20%). Alternatively, a toluene solution (20 mL) of 6-o-Tol (prepared in situ by reaction of the pyrimidinium salt [6-o-TolH]BF₄ (345 mg, 1.30 mmol) and K[N(SiMe₃)₂] (257 mg, 1.29 mmol)) was added to a toluene solution (10 mL) of Ni(PPh₃)₂Br₂ (959 mg, 1.29 mmol). The mixture was stirred at room temperature for 1 h to give a dark purple solution. After cannula filtration, the volatiles were removed under vacuum, and the residue was washed with hexane (15 mL). The resulting purple-green residue was recrystallized repeatedly from toluene/hexane to remove all traces of [6-o-TolH][Ni(PPh₃)Br₃] (see Supporting Information) and leave just 10. Yield 141 mg (15%). ³¹P{¹H}NMR (162 MHz, CD₂Cl₂, 25 °C): δ 17.3 (s), 16.6 (s). ¹³C{¹H}NMR (126 MHz, CD₂Cl₂, 25 °C): δ 194.1 (d, ²J_{CP} = 122 Hz, NCN), 193.7 (d, ²J_{CP} = 123 Hz, NCN), 146.3 (s, N-C), 145.9 (s, N-C), 137.7 (s), 136.9 (s), 135.2 (br m), 132.9 (s), 132.6 (s), 131.9 (s), 131.7 (s), 129.7 (s), 128.6 (s), 128.4 (s), 127.8 (s), 127.7 (s), 127.0 (s), 126.7 (s), 49.4 (s, NCH₂), 49.0 (s, NCH₂), 21.3 (s, NCH₂CH₂), 20.2 (s, o-CH₃), 19.8 (s, o-CH₃). Anal. calcd (found) for C₃₆H₃₅N₂PBr₂Ni (%): C, 58.03 (57.85), H 4.73 (4.83), N 3.76 (3.69).

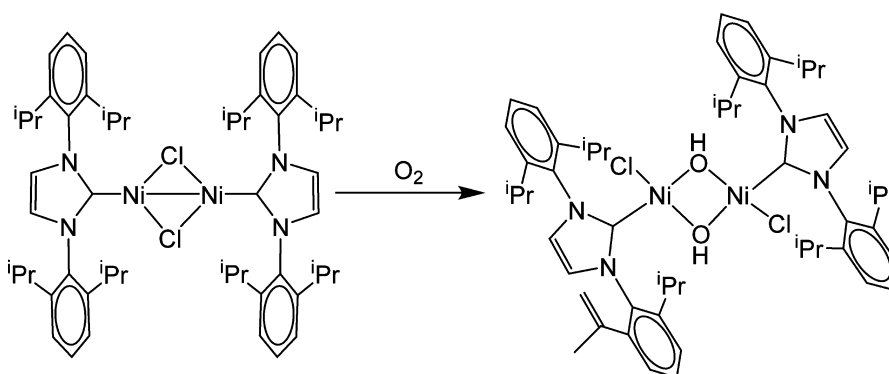
Ni(7-o-Tol)(PPh₃)Br₂ (11). Compound 11 was synthesized similarly to 10, by reaction of Ni(7-o-Tol)(PPh₃)Br (47 mg, 0.069 mmol) with O₂ to give 10 mg (38%) of 11. The alternative route to 10 could also be applied to 11 starting with Ni(PPh₃)₂Br₂ and addition of a toluene solution (20 mL) of 7-o-Tol (prepared in situ by reaction of [7-o-TolH]BF₄ (200 mg, 0.55 mmol) with K[N(SiMe₃)₂] (110 mg, 0.55 mmol)) to a toluene solution (5 mL) of Ni(PPh₃)₂Br₂ (406 mg, 0.55 mmol). Yield: 47 mg (12%). ³¹P{¹H}NMR (162 MHz, CDCl₃, 25 °C): δ 21.4 (s), 21.3 (s), 20.3 (s), 17.5 (s), 16.7 (s). ¹³C{¹H}NMR (100 MHz, C₆D₆, 25 °C): δ 206.7 (d, ²J_{CP} = 123 Hz, NCN), 148.7 (s), 147.4 (s), 147.1 (s), 137.4 (s), 137.2 (s), 135.6 (s), 135.5 (s), 133.0 (s), 131.6 (s), 129.2 (s), 127.6 (d, J_{CP} = 9 Hz), 126.7 (s), 56.0 (s, NCH₂), 55.9 (s, NCH₂), 55.7 (s, NCH₂), 55.6 (s, NCH₂), 25.5 (s, NCH₂CH₂), 23.7 (s, NCH₂CH₂), 21.4 (s, o-CH₃), 20.8 (s, o-CH₃), 20.6 (s, o-CH₃), 20.1 (s, o-CH₃). Anal. calcd (found) for C₃₇H₃₇N₂PBr₂Ni (%): C, 58.69 (58.54), H 4.93 (5.05), N 3.69 (3.60).

X-ray Crystallography. Single crystals of compounds 3–5, 7, 10, and 11 were analyzed using a Nonius Kappa CCD diffractometer. Data were collected at –123 °C using Mo K α radiation throughout. Details of the data collections, solutions and refinements are given in Table 1. The structures were solved using SHELXS-97¹³ and refined using full-

Scheme 2



Scheme 3



matrix least-squares in SHELXL-97.¹³ Refinements were generally straightforward and notable points follow.

The hydrogen atoms on the hydroxyl groups in **3** and **4** were readily located and refined at distances of 0.9 and 0.98 Å from the relevant parent oxygen atoms, respectively, in these structures. Halide disorder (80:20 ratio) of chloride versus bromide was accommodated in the model for **5**. The ADPs for the associated pairs of fractional occupancy atoms, at each ligand site, were refined subject to being similar. In **10**, the tolyl ring based on C(12) exhibited disorder in a 75:25 ratio. To assist convergence, the arising fractional occupancy rings were refined as rigid hexagons and ADP restraints were also applied. It is likely that there is also some similar disorder associated with the tolyl ring based on C(5) in this structure, but despite copious efforts, a model to further resolve this region of the electron density map could not be attained.

Crystallographic data for compounds **3–5**, **7**, **10**, **11**, and $\text{Ni}(\text{O}=\text{PPh}_3)_2\text{Br}_2$ (Supporting Information only) have been deposited with the Cambridge Crystallographic Data Centre as supplementary publications CCDC 972766 (**3**), 972767 (**4**), 972768 (**5**), 972769 (**7**), 905841 (**10**), 905840 (**11**) and 974548 ($\text{Ni}(\text{O}=\text{PPh}_3)_2\text{Br}_2$). Copies of the data can be obtained free of charge on application to

CCDC, 12 Union Road, Cambridge CB2 1EZ, UK [fax(+44) 1223 336033, e-mail: deposit@ccdc.cam.ac.uk].

RESULTS AND DISCUSSION

Conversion of $\text{Ni}(\text{6-Mes})(\text{PPh}_3)\text{Br}$ and $\text{Ni}(\text{7-Mes})(\text{PPh}_3)\text{Br}$ to $\text{Ni}(\text{II})$ Dimers with Oxidized N-Mes Ligands.

Addition of 1 atm of O_2 to yellow THF solutions of either $\text{Ni}(\text{6-Mes})(\text{PPh}_3)\text{Br}$ (**1**) or $\text{Ni}(\text{7-Mes})(\text{PPh}_3)\text{Br}$ (**2**) led to instantaneous color changes to purple. Upon removal of the solvent and recrystallization of the resulting residues from THF/hexane or CH_2Cl_2 /hexane, purple crystals of the $\text{Ni}(\text{II})$ complexes $\text{Ni}(\text{6-Mes})(\text{Br})(\mu\text{-OH})(\mu\text{-O-6-Mes}')\text{NiBr}$ (**3**) and $\text{Ni}(\text{7-Mes})(\text{Br})(\mu\text{-OH})(\mu\text{-O-7-Mes}')\text{NiBr}$ (**4**) were isolated (Scheme 2). These products result from the oxidation of a C–H bond¹⁴ in one of the *ortho*-methyl groups on the NHCs to afford dinuclear species with bridging aryloxy and hydroxy ligands.^{15,16} The most likely source of hydrogen in the hydroxy ligands is the oxidized methyl arm of the carbene.¹⁶

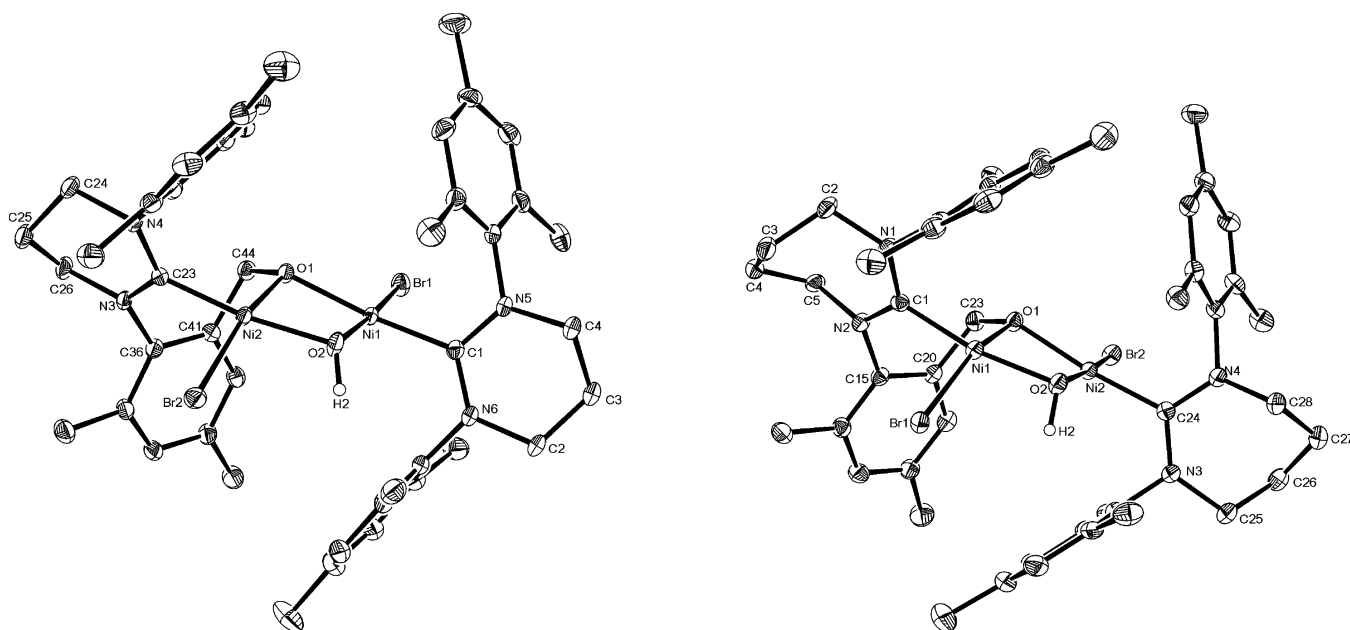


Figure 1. Molecular structures of **3** (left) and **4** (right). Ellipsoids are shown at the 30% level. Hydrogen atoms except for μ -OH are removed for clarity. Selected bond lengths (Å) and angles (deg) in **3**: Ni(1)–C(1) 1.883(4), Ni(2)–C(23) 1.856(3), Ni(1)–O(1) 1.926(2), Ni(1)–O(2) 1.869(3), Ni(2)–O(1) 1.892(2), Ni(2)–O(2) 1.890(2), O(1)–C(44) 1.443(4), Ni(1)–O(1)–Ni(2) 97.53(11), O(1)–C(44)–C(41) 111.4(3). Selected bond lengths (Å) and angles (deg) in **4**: Ni(1)–C(1) 1.878(4), Ni(2)–C(24) 1.896(4), Ni(1)–O(1) 1.889(3), Ni(1)–O(2) 1.896(3), Ni(2)–O(1) 1.936(3), Ni(2)–O(2) 1.878(3), O(1)–C(23) 1.437(5), Ni(1)–O(1)–Ni(2) 98.00(13), O(1)–C(23)–C(20) 112.6(4).

Our findings show some parallels to earlier work from Sigman's group, who reported that addition of O_2 to the Ni(I) dimer shown in Scheme 3 containing the bulky IPr ligand¹⁷ also resulted in oxidation of the N-substituent, although in this case with dehydrogenation of an ⁱPr substituent rather than hydroxylation.^{2h,18}

The X-ray crystal structures of **3** and **4** are shown in Figure 1. In both cases, the four-coordinate Ni centers display distorted square planar geometries. This may reflect the strain imposed by the bridging OCH_2 -aryl group, which contributes to some acute O–Ni–O bond angles (**3**, 80.18(10)° and 80.55(10)°; **4**, 80.13(13)° and 79.40(13)°). The Ni–O distances in the central $Ni_2(\mu-OR)(\mu-OH)$ units are also asymmetric; the longest distances are found between the nonoxidized NHC bound Ni and μ - OCH_2 -aryl (**3**, Ni(1)–O(1) 1.926(2) Å; **4**, Ni(2)–O(1) 1.936(3) Å), the shortest Ni–O bond lengths being from the same Ni centers to the μ -OH groups (**3**, Ni(1)–O(2) 1.869(3) Å; **4**, Ni(2)–O(2) 1.878(4) Å). It is notable that, in **3**, deviation of the carbene nitrogen atoms from the mean plane of the surrounding bonded carbon atoms is maximized in the case of that bonded to the hydroxylated mesityl ring (0.11 Å for N(3) relative to an average of 0.02 Å for N(4), N(5), and N(6)). These data reflect a distortion from idealized sp^2 geometry at N(3), about which strain is optimal. A comparative observation is evident in **4** where the distance of N(2) from the mean plane of the surrounding bonded carbon atoms is 0.16 Å.

The presence of a hydroxy group in both **3** and **4** was confirmed by ¹H NMR and IR spectroscopy. Thus, for **3**, we observed a low frequency proton signal (δ –6.2 (CD₂Cl₂); δ –8.4 (C₆D₆)) consistent with Ni–OH^{18,19} and a μ -OH stretch at 3412 cm^{–1}. Both signals disappeared upon addition of D₂O. The remainder of the ¹H NMR spectrum of **3** yielded very little interpretable information; in CD₂Cl₂ in particular, only a series of broad, partially overlapping singlet resonances were observed

(see Supporting Information), which we could not assign to specific groups. The spectrum of **4** was even broader and therefore even less diagnostic (Supporting Information). These spectra are discussed further below. Neither compound proved to be soluble enough in acetone, acetonitrile, benzene, toluene, dichloromethane, or even C₆H₅F to afford helpful ¹³C NMR spectra (Supporting Information). In particular, we were unable to observe Ni–C_{NHC} resonances in either case.

Complex **3** did exhibit slightly greater solubility in pyridine or pyridine doped CH₂Cl₂ (5 equiv of C₅H₅N), although in both cases, this resulted in noticeably more orange colored solutions. Upon layering the CH₂Cl₂/C₅H₅N sample with hexane, a small number of purple crystals were formed, which were shown by X-ray crystallography to be Ni(Br)(μ -O-6-Mes')₂NiBr (**5**; Figure 2) resulting from oxidation of a C–H bond in each of the 6-Mes ligands.²⁰ The coordination spheres of the two identical square planar Ni centers consist of an oxidized 6-Mes ligand, two μ -OR linkages and an 80:20 mixture of disordered Br and Cl ligands, the latter presumably arising from the CH₂Cl₂ used as solvent. The oxidized arms of the 6-Mes ligands are in a *syn* arrangement about the planar $Ni_2(\mu-OR)_2$ core with Ni–O distances comparable to those in **3**. In contrast to **3** and **4**, structural distortions of the nitrogen atoms attached to the oxidized mesityl groups are marginal.

Despite many efforts, we were unable to produce **5** in greater yields for more complete characterization. However, ESI-TOF mass spectral analysis of MeCN solutions of crystalline material produced from reacting **1** with O_2 gave an isotope pattern consistent with the presence of both **3** and **5** (see Supporting Information). When the ¹H NMR spectrum of **3** described above was analyzed further, we noted that integration of the remainder of the spectrum relative to the Ni–OH resonance afforded a greater number of protons than could be accounted for by the presence of **3** alone. Thus, while **3** can be isolated and characterized as a pure material in the solid state, upon

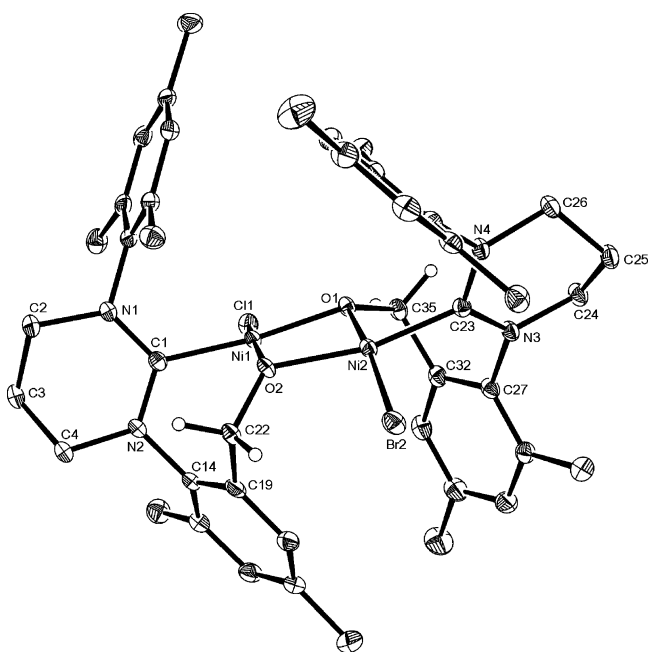


Figure 2. Molecular structure of **5**. Ellipsoids are shown at the 30% level. Hydrogen atoms (except for those on the oxidized methyl arms) are removed for clarity. Selected bond lengths (Å) and angles (deg): Ni(1)–C(1) 1.868(2), Ni(2)–C(23) 1.872(2), Ni(1)–O(1) 1.9204(14), Ni(1)–O(2) 1.8806(15), Ni(2)–O(1) 1.8873(14), Ni(2)–O(2) 1.9166(14), Ni(1)–O(1)–Ni(2) 99.48(6), Ni(1)–O(2)–Ni(2) 99.86(7).

dissolution, it appears to be prone to further functionalization of the second mesityl substituent and thus formation of **5** in solution. In an effort to confirm this, X-ray unit cell parameters for six separate crystals from a batch of material isolated from the reaction of **1** and O₂ were measured. Because the cell parameters, in all cases, matched those of just **3**, it would appear that the crystalline material consists overwhelmingly of this one compound. However, the ¹H NMR spectrum recorded upon dissolution of the remaining crystals again integrated to too many protons than could be accounted for by just **3** alone.

Identical observations were made on the 7-Mes analogue **4**. Mass spectra of solutions of **4** showed an isotope pattern (Supporting Information) consistent with the presence of **4** and the doubly oxidized analogue **6** (Scheme 2).²¹ The same crystal picking method of analysis as above once more pointed only to the presence of **4** in the solid state, whereas NMR analysis indicated the presence of more than this one species in solution.

UV–Visible Spectroscopic Studies on the Reaction of **1 with O₂.** The room temperature electronic absorption spectrum of **3** measured in THF solution contained a single absorption band at λ_{max} = 362 nm (*ε* = 474 M cm^{−1}; this value is based on the assumption that **3** is the only species present). In an effort to probe the mechanism of formation of **3** in more detail, **1** was dissolved in THF at −83 °C, 1 mL of air was added at this temperature, and the reaction was monitored by UV–vis spectroscopy (Figure 3). After 6 min reaction time, no further change was observed in the UV–vis spectrum, revealing that the reaction was complete. The final spectrum obtained is very similar to that of **3** suggesting that this is the major species of the reaction of **1** + O₂. However, it is likely that the bis-*μ*-alkoxy complex **5** would have a very similar UV–vis spectrum due to the very similar chromophores. Indeed, evidence for the

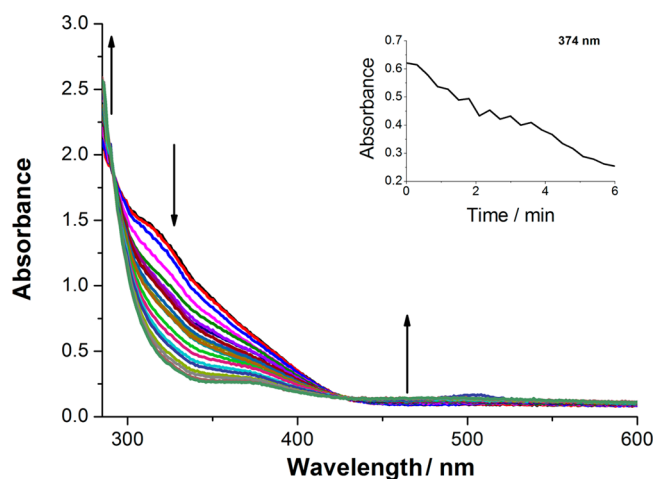


Figure 3. UV–vis monitoring of the reaction of 1 mL of air with 0.5 mM **1** at −83 °C in THF over a period of 6 min. Measurements were taken every 18 s. The inset shows the absorbance vs. time plot at 374 nm.

formation of multiple species in the reaction was suggested by the kinetic analysis where the singular value decomposition (SVD) analysis shows the presence of at least three eigenvectors. It is therefore not possible to develop a simple kinetic model even if at first sight nice isosbestic points are observed at 290 and 420 nm.

The formation of **3** from **1** and oxygen suggests the formation of highly reactive high oxidation state Ni bis-oxo or peroxy species that further evolve toward the formation of **3** and **5**. Attempts to detect such intermediates by carrying out the reaction at different temperatures proved unsuccessful.

Synthesis of a Ni(II) Diamidocarbene Complex and Its Reactivity with O₂. In an attempt to retard the rate of mesityl group oxidation which might allow the observation of intermediates, the novel, less electron-rich diamidocarbene complex Ni(6-MesDAC)(PPh₃)Br (**7**) was prepared and reacted with O₂. The synthesis of **7** employed the same method as used for the synthesis of **1** and **2**,^{24,9} namely, comproportionation of Ni(0) (Ni(cod)₂) and Ni(II) (Ni(PPh₃)₂Br₂) in the presence of the free carbene. This gave **7** in 60% yield (Scheme 4).

The NMR spectra of **7** were in agreement with those found for **1** and **2**. A series of broad resonances were observed between δ 11 and −1 in the proton NMR spectrum, while there was no signal at all present in the ³¹P{¹H} spectrum (Supporting Information). The X-ray structure of **7** (Figure 4) was isostructural with that of **1**, although the Ni–C bond length was significantly shorter (1.8702(18) Å; cf. 1.942(2) Å in **1**), presumably as a result of the enhanced π-acceptor character of the diamidocarbene.²²

An immediate but quite different color change took place upon adding O₂ to a THF solution of **7**. Purple crystals of the compound dissolved to give dark orange-yellow solutions, which became virtually colorless upon O₂ addition, suggestive of different species from **3** and **4** being formed. Attempted crystallization from either CH₂Cl₂/hexane or THF/hexane afforded a creamy-green precipitate, from which a small number of green and colorless crystals were isolated and manually separated. Using a combination of X-ray crystallography and NMR spectroscopy, these were shown to be the Ni(II) phosphine oxide complex Ni(O=PPh₃)₂Br₂ (see Supporting

Scheme 4

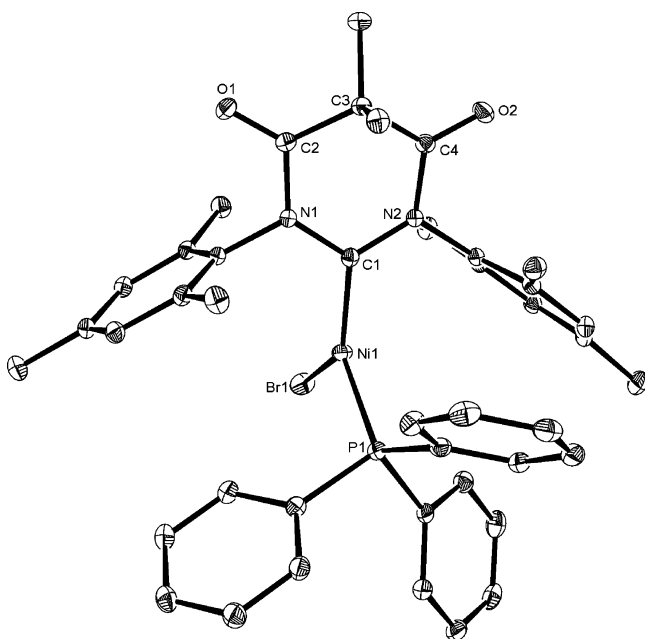
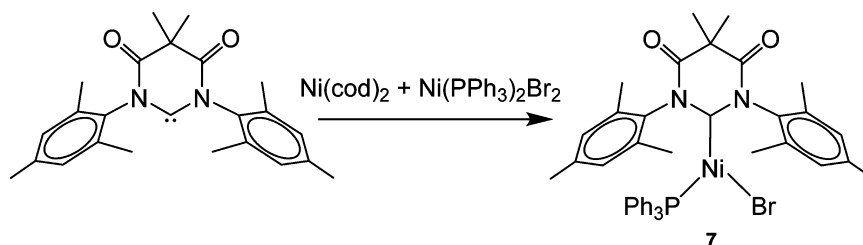


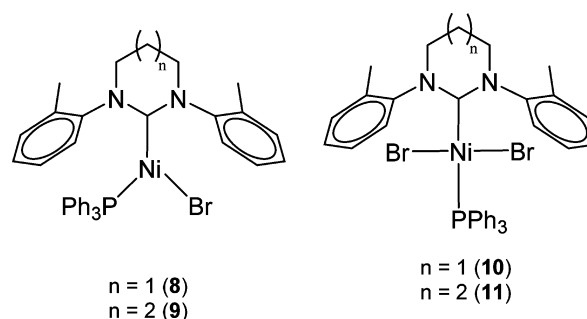
Figure 4. Molecular structure of **7**. Ellipsoids are shown at the 30% level. All hydrogen atoms are removed for clarity. Selected bond lengths (Å) and angles (deg): Ni(1)–C(1) 1.8702(18), Ni(1)–P(1) 2.2614(5), Ni(1)–Br(1) 2.3029(3), C(1)–Ni(1)–P(1) 118.99(5), C(1)–Ni(1)–Br(1) 127.66(5), P(1)–Ni(1)–Br(1) 113.352(16).

Information for structure)²³ and urea (6-MesDAC)=O, respectively.¹²

Reactivity of Less Bulky Ni(II) RE-NHC Complexes with O₂. In light of the effect seen upon changing from a diamino- to a diamidocarbene, we also probed the impact of using less-bulky *ortho*-tolyl substituted RE-NHCs. As for **7**, addition of O₂ to both the new six-membered ring species Ni(6-*o*-Tol)(PPh₃)Br (**8**) and the previously reported⁹ larger ring analogue Ni(7-*o*-Tol)(PPh₃)Br (**9**) did not result in oxidation of the NHC ligands. Instead, the mononuclear Ni(II) dibromide complexes Ni(6-*o*-Tol)(PPh₃)Br₂ and Ni(7-*o*-Tol)(PPh₃)Br₂ (**10** and **11**) were isolated (Scheme 5). The low yields (20% and 38% respectively) of these compounds and their formation by halide redistribution means that other species (which we have been unable to identify) must be formed in the reaction in order to bring about mass balance.

Unambiguous characterization of **10** and **11** was facilitated by an independent synthesis involving the treatment of Ni(PPh₃)₂Br₂ with an equimolar amount of the corresponding 6- or 7-*o*-Tol ligand.^{24,25} The crystal structures of **10** and **11** (Figure 5) showed the expected square planar Ni geometries with *trans* bromide ligands. The Ni–C_{NHC} distances of 1.910(5) Å (**10**) and 1.905(3) Å (**11**) were comparable to that reported for *trans*-Ni(IPr)(PPh₃)Cl₂ (1.912(4) Å),²⁵ which is one of the

Scheme 5



few other examples of Ni(NHC)(PR₃)(halide)₂ complexes reported in the literature.

Surprisingly, **10** showed two resonances in the ³¹P{¹H} NMR spectrum (CD₂Cl₂) at δ 17.3 and 16.6 in a ratio of ca. 1:1.9 (Supporting Information). Assignment of these two species as *cis*- and *trans*-isomers could be excluded by the appearance of large (122 Hz) *trans*-¹³C/³¹P coupling on both of the carbene resonances seen in the corresponding ¹³C{¹H} NMR spectrum. In the case of **11**, five phosphorus signals were seen in C₆D₆ at δ 21.4, 21.3, 20.3, 17.5, and 16.7 (Supporting Information), although only the two lowest frequency signals were of any significant intensity (approximate ratio 1:2:1:38:13). A ³¹P–³¹P EXSY spectrum revealed exchange between the resonances at δ 17.5 and 16.7 and a separate exchange process involving the three smaller signals at δ 21.4, 21.3, and 20.3 (Supporting Information).

The formation of rotamers affords the most likely explanation for the appearance of the multiple phosphorus signals in the spectra of the two compounds. Indeed, Cavell's group have proposed rotamers (differing in *syn*- versus *anti*-arrangements of the *o*-Me groups on the NHC) to account for the appearance of multiple signals in the proton NMR spectrum of Rh(7-*o*-Tol)(cod)Cl.²⁶

Redox Properties of 1, 2, and 7–9. In an effort to rationalize the different reactivities of the mesityl and tolyl diaminocarbene and diamidocarbene Ni(I) complexes toward O₂, their redox properties have been probed by means of cyclic voltammetry. The CVs of complexes **1** and **7** (Figure 6) show the presence of a chemically irreversible oxidation in the anodic region and a chemically irreversible reduction in the cathodic region. Similar behavior was observed for **2**, while **8** and **9** showed two irreversible reductions (Supporting Information). The E_{p,a} and E_{p,c} values found for the five complexes are given in Table 2. As already mentioned, in all cases the redox processes are chemically irreversible, and this precludes the extraction of accurate thermodynamic potentials. However, since all the mononuclear complexes studied have very similar molecular structures, especially around the Ni center, indicative trends can be deduced.

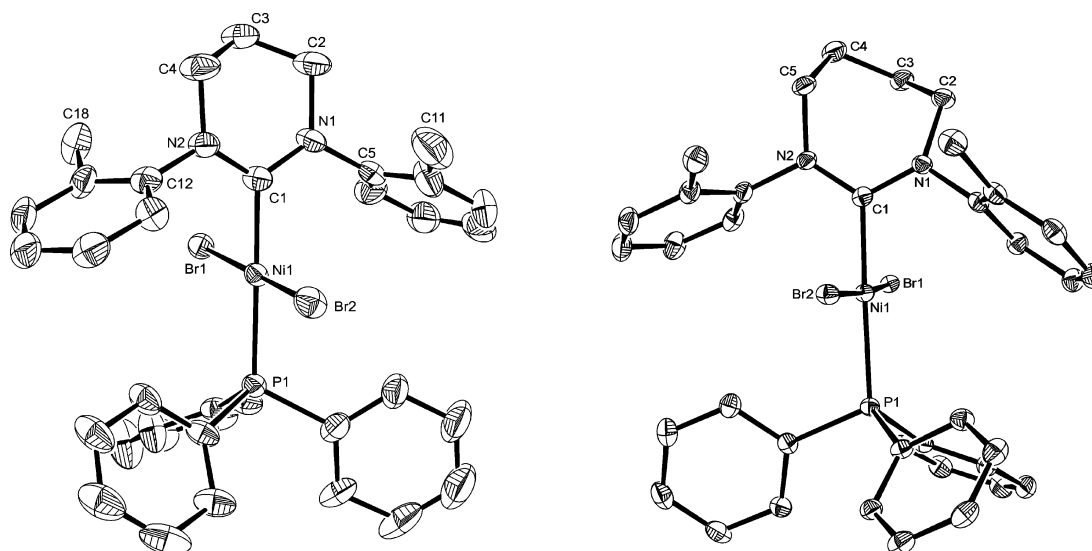


Figure 5. Molecular structures of **10** (left) and **11** (right). Ellipsoids are shown at the 30% level. Hydrogen atoms are removed for clarity. Selected bond lengths (Å) and angles (deg) in **10**: Ni(1)–C(1) 1.910(5), Ni(1)–P(1) 2.2505(15), Ni(1)–Br(1) 2.3026(8), Ni(1)–Br(2) 2.3122(9), C(1)–Ni(1)–P(1) 179.26(18), Br(1)–Ni(1)–Br(2) 175.82(4). Selected bond lengths (Å) and angles (deg) in **11**: Ni(1)–C(1) 1.905(3), Ni(1)–P(1) 2.2615(8), Ni(1)–Br(1) 2.4013(4), Ni(1)–Br(2) 2.3511(4), C(1)–Ni(1)–P(1) 177.44(9), Br(1)–Ni(1)–Br(2) 174.192(19).

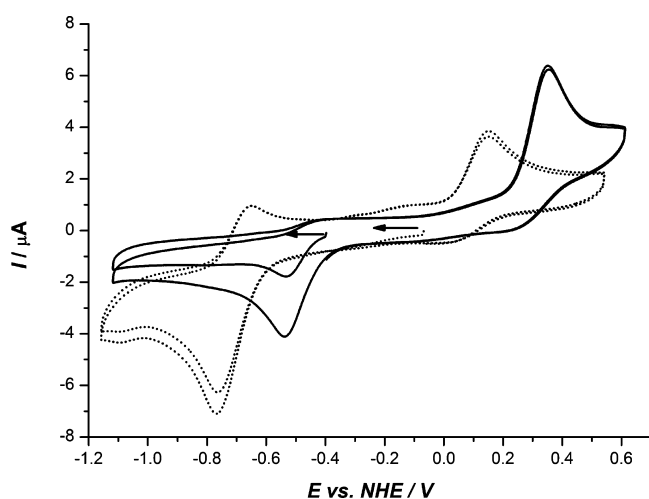


Figure 6. Cyclic voltammograms for complexes **1** (solid line) and **7** (dashed line) at 100 mV/s scan rate vs. NHE. The arrow indicates the initial scanning potential and the scan direction.

Table 2. Anodic and Cathodic Redox Waves Observed for Ni(I) Complexes

Ni(I) complex	$E_{p,a}$ (V vs NHE)	$E_{p,c}$ (V vs NHE)
1	0.35	-0.54
2	0.48	-0.49
7	0.15	-0.77
8	0.25	-0.68, -1.19
9	0.20	-0.72, -1.08

The anodic potentials shown in Table 2 do not follow a regular trend based on the induction effects expected by increasing the number of methylene units in the carbene ligand backbones or by increasing the number of Me groups (tolyl to mesityl) in the N-substituents. It is also surprising that **7**, containing the diamidocarbene, displays one of the lowest $E_{p,a}$ values, together with **9**. However, the most interesting feature that can be extracted from these data is the fact that complexes

1 and **2**, which have the highest redox potentials by far, are the ones that undergo oxidation involving O atom transfer from O_2 . On the other hand, the rest of the complexes with much lower redox potentials undergo oxidation primarily by outer sphere electron transfer (OSET) giving basically Ni(II) complexes with no oxygen incorporated into the final products. This suggests that complexes that are much more difficult to oxidize by OSET (**1** and **2**) find a lower energy pathway involving O atom transfer from O_2 , hence the formation of the hydroxy-aryloxy bridged Ni(II) complexes.

SUMMARY AND CONCLUSIONS

The reactivity of the three-coordinate Ni(I) ring-expanded NHC complexes Ni(RE-NHC)(PPh₃)Br toward O_2 has been investigated. A range of Ni(II) products are formed, which prove to be dependent upon the stereoelectronic properties of the carbene. In the cases of complexes with N-mesityl substituted NHCs (**1** and **2**), oxidation of a C–H bond leads to dimeric Ni(II) products containing μ -alkoxy ligands. This reactivity appears to correlate with the high redox potentials of **1** and **2** determined by cyclic voltammetry. Attempts to probe the mechanism of oxidation and detect reaction intermediates by UV–vis spectroscopy have been thwarted by the remarkably facile nature of the process, which appears to be complete within a few minutes even at $-83^\circ C$. These low temperature experiments along with mass spectrometry provide direct evidence for further oxidation of the second N-mesityl group taking place. This has been confirmed by the structural characterization of the 6-Mes derivative Ni(Br)(μ -O-6-Mes')₂NiBr (**5**), although the exact circumstances under which this secondary reaction takes place are unclear at this time.

In an effort to slow the rate of oxidation through the use of less bulky *N*-*o*-Tol or more π -accepting diamidocarbene containing precursors, different reaction pathways were found resulting in the isolation of Ni(II) complexes arising predominantly from ligand redistribution and degradation. That such different reactivity takes place upon making the relatively small change of *N*-mesityl to *N*-*o*-tolyl groups at first

hand seems somewhat surprising, although the CV measurements show some marked differences in redox properties. We hope that the synthesis of additional derivatives of the Ni(RE-NHC)(PPh₃)Br complexes through alteration of the phosphine or substitution of the bromide ligand will aid in developing a clearer understanding of the oxidation chemistry.

■ ASSOCIATED CONTENT

■ Supporting Information

NMR spectra of **3**, **4**, **7**, **8**, **10**, and **11**, mass spectra for **3**–**6**, X-ray structure of Ni(O=PPh₃)₂Br₂, characterization of [6-*o*-TolH][Ni(PPh₃)Br₃], and electrochemical measurements on **2**, **8**, and **9**. This material is available free of charge via the Internet at <http://pubs.acs.org>.

■ AUTHOR INFORMATION

Corresponding Author

*E-mail: chsmkw@bath.ac.uk.

Notes

The authors declare no competing financial interest.

■ ACKNOWLEDGMENTS

We acknowledge the University of Bath (Excellent Studentship Award to RCP) and MINECO (CTQ2013-49075-R) for financial support. Dr. Anneke Lubben and Dr. John Lowe are thanked for help with mass spectrometry and NMR, respectively, while Mr. Lee Collins is thanked for samples of 6-MesDAC.

■ REFERENCES

- (1) (a) Ugo, R. *Coord. Chem. Rev.* **1968**, *3*, 319. (b) Jolly, P. W.; Jonas, K. *Angew. Chem., Int. Ed.* **1968**, *7*, 731. (c) Jolly, P. W. In *Comprehensive Organometallic Chemistry*; Wilkinson, G., Stone, F. G. A., Abel, E. W., Eds.; Pergamon: Oxford, U.K., 1982; Vol. 6, p 37. (d) Sacconi, L.; Mani, F.; Bencini, A. In *Comprehensive Coordination Chemistry*; Wilkinson, G., Gillard, R. D., McCleverty, J. A., Eds.; Pergamon: Oxford, U.K., 1987; Vol. 5, p 1. (e) Kubiak, C. P. In *Comprehensive Organometallic Chemistry II*; Abel, E. W., Stone, F. G. A., Wilkinson, G., Eds.; Pergamon: Oxford, U.K., 1995; Vol. 9, p 1. (f) Meyer, F.; Kozłowski, H. In *Comprehensive Coordination Chemistry II*; McCleverty, J. A., Meyer, T. J., Eds.; Pergamon: Oxford, U.K., 2004; Vol. 6, p 497. (g) Kubiak, C. P.; Simón-Manso, E. In *Comprehensive Organometallic Chemistry III*; Crabtree, R. H., Mingos, D. M. P., Eds.; Pergamon: Oxford, U.K., 2007; Vol. 8, p 1.
- (2) (a) Bradley, D. C.; Hursthouse, M. B.; Smallwood, R. J.; Welch, A. J. *J. Chem. Soc., Chem. Commun.* **1972**, 872. (b) Eaborn, C.; Hill, M. S.; Hitchcock, P. B.; Smith, J. D. *Chem. Commun.* **2000**, 691. (c) Mindiola, D. J.; Hillhouse, G. L. *J. Am. Chem. Soc.* **2001**, *123*, 4623. (d) Melenkivitz, R.; Mendiola, D. J.; Hillhouse, G. L. *J. Am. Chem. Soc.* **2002**, *124*, 3846. (e) Kitiachvili, K. D.; Mendiola, D. J.; Hillhouse, G. L. *J. Am. Chem. Soc.* **2004**, *126*, 10554. (f) Bai, G.; Wei, P.; Stephan, D. W. *Organometallics* **2005**, *24*, 5901. (g) Eckert, N. A.; Dinescu, A.; Cundari, T. R.; Holland, P. R. *Inorg. Chem.* **2005**, *44*, 7702. (h) Dible, B. R.; Sigman, M. S.; Arif, A. M. *Inorg. Chem.* **2005**, *44*, 3774. (i) Chen, Y.; Syu-Seng, C.; Zargarian, D. *Angew. Chem., Int. Ed.* **2005**, *44*, 7721. (j) Kogut, E.; Wiencko, H. L.; Zhang, L.; Cordeau, D. E.; Warren, T. H. *J. Am. Chem. Soc.* **2005**, *127*, 11248. (k) Keen, A. L.; Doster, M.; Johnson, S. A. *J. Am. Chem. Soc.* **2007**, *129*, 810. (l) Ingleson, M. J.; Fullmer, B. C.; Buschhorn, D. T.; Fan, H.; Pink, M.; Huffman, J. C.; Caulton, K. G. *Inorg. Chem.* **2008**, *47*, 407. (m) Laskowski, C. A.; Hillhouse, G. L. *J. Am. Chem. Soc.* **2008**, *130*, 13846. (n) Pfirrmann, S.; Limberg, C.; Herwig, C.; Stösser, R.; Ziemer, B. *Angew. Chem., Int. Ed.* **2009**, *48*, 3357. (o) Laskowski, C. A.; Hillhouse, G. L. *Organometallics* **2009**, *28*, 6114. (p) Ito, M.; Matsumoto, T.; Tatsumi, K. *Inorg. Chem.* **2009**, *48*, 2215. (q) Davies, C. J. E.; Page, M. J.; Ellul, C. E.; Mahon, M. F.; Whittlesey, M. K. *Chem. Commun.* **2010**, 46, 5151. (r) Velian, A.; Lin, S.; Miller, A. J. M.; Day, M. W.; Agapie, T. *J. Am. Chem. Soc.* **2010**, *132*, 6296. (s) Iluc, V. M.; Hillhouse, G. L. *J. Am. Chem. Soc.* **2010**, *132*, 11890. (t) Iluc, V. M.; Hillhouse, G. L. *J. Am. Chem. Soc.* **2010**, *132*, 15148. (u) Jones, C.; Schulten, C.; Fohlmeister, L.; Stasch, A.; Murray, K. S.; Moubaraki, B.; Kohl, S.; Ertem, M. Z.; Gagliardi, L.; Cramer, C. J. *Chem.—Eur. J.* **2011**, *17*, 1294. (v) Chao, S. T.; Lara, N. C.; Lin, S.; Day, M. W.; Agapie, T. *Angew. Chem., Int. Ed.* **2011**, *50*, 7529. (w) Beck, R.; Shoshani, M.; Krasinkiewicz, J.; Hatnean, J. A.; Johnson, S. A. *Dalton Trans.* **2013**, 42, 1461. (x) Lipschutz, M. I.; Yang, X.; Chatterjee, R.; Tilley, T. D. *J. Am. Chem. Soc.* **2013**, *135*, 15298. (y) Poulten, R. C.; Page, M. J.; Algarra, A. G.; Le Roy, J. J.; López, I.; Carter, E.; Llobet, A.; Macgregor, S. A.; Mahon, M. F.; Murphy, D. M.; Murugesu, M.; Whittlesey, M. K. *J. Am. Chem. Soc.* **2013**, *135*, 13640. (z) Wu, J.; Nova, A.; Balcells, D.; Brudvig, G. W.; Dai, W.; Guard, L. M.; Hazari, N.; Lin, P.-H.; Pokhrel, R.; Takase, M. K. *Chem.—Eur. J.* **2014**, *20*, 5327.
- (3) For recent reviews, see: (a) Kieber-Emmons, M. T.; Riordan, C. G. *Acc. Chem. Res.* **2007**, *40*, 618. (b) Yao, S. L.; Driess, M. *Acc. Chem. Res.* **2012**, *45*, 276.
- (4) For representative examples, see: (a) Mandimutsira, B. S.; Yamarik, J. L.; Brunold, T. C.; Gu, W.; Cramer, S. P.; Riordan, C. G. *J. Am. Chem. Soc.* **2001**, *123*, 9194. (b) Fujita, K.; Schenker, R.; Gu, W. W.; Brunold, T. C.; Cramer, S. P.; Riordan, C. G. *Inorg. Chem.* **2004**, *43*, 3324. (c) Kieber-Emmons, M. T.; Schenker, R.; Yap, G. P. A.; Brunold, T. C.; Riordan, C. G. *Angew. Chem., Int. Ed.* **2004**, *43*, 6716. (d) Pfirrmann, S.; Limberg, C.; Ziemer, B. *Dalton Trans.* **2008**, 6689. (e) Yao, S.; Bill, E.; Milsmann, C.; Wieghardt, K.; Driess, M. *Angew. Chem., Int. Ed.* **2008**, *47*, 7110. (f) Pfirrmann, S.; Yao, S.; Ziemer, B.; Stösser, R.; Driess, M.; Limberg, C. *Organometallics* **2009**, *28*, 6855. (g) Anderson, J. S.; Iluc, V. M.; Hillhouse, G. L. *Inorg. Chem.* **2010**, *49*, 10203. (h) Horn, B.; Pfirrmann, S.; Limberg, C.; Herwig, C.; Braun, B.; Mebs, S.; Metzinger, R. Z. *Anorg. Allg. Chem.* **2011**, 637, 1169. (i) Chen, Y.; Sakaki, S. *Inorg. Chem.* **2013**, *52*, 13146. (j) Horn, B.; Limberg, C.; Herwig, C.; Braun, B. *Chem. Commun.* **2013**, 49, 10923. (k) Laskowski, C. A.; Morello, G. R.; Saouma, C. T.; Cundari, T. R.; Hillhouse, G. L. *Chem. Sci.* **2013**, *4*, 170.
- (5) (a) Evans, D. J. *Coord. Chem. Rev.* **2005**, *249*, 1582. (b) Ragsdale, S. W. *Chem. Rev.* **2006**, *106*, 3317. (c) Can, M.; Armstrong, F. A.; Ragsdale, S. W. *Chem. Rev.* **2014**, *114*, 4149.
- (6) (a) Harmer, J.; Finazzo, C.; Piskorski, R.; Ebner, S.; Duin, E. C.; Goenrich, M.; Thauer, R. K.; Reiher, M.; Schweiger, A.; Hinderberger, D.; Jaun, B. *J. Am. Chem. Soc.* **2008**, *130*, 10907. (b) Li, X.; Telser, J.; Kunz, R. C.; Hoffman, B. M.; Gerfen, G.; Ragsdale, S. W. *Biochemistry* **2010**, *49*, 6866. (c) Scheller, S.; Goenrich, M.; Boecher, R.; Thauer, R. K.; Jaun, B. *Nature* **2010**, *465*, 606. (d) Nishigaki, J.; Matsumoto, T.; Tatsumi, K. *Inorg. Chem.* **2012**, *51*, 5173.
- (7) Scheller, S.; Goenrich, M.; Mayr, S.; Thauer, R. K.; Jaun, B. *Angew. Chem., Int. Ed.* **2010**, *49*, 8112.
- (8) (a) Ragsdale, S. W.; Kumar, M. *Chem. Rev.* **1996**, *96*, 2515. (b) Bender, G.; Stich, T. A.; Yan, L.; Britt, R. D.; Cramer, S. P.; Ragsdale, S. W. *Biochemistry* **2010**, *49*, 7516. (c) Horn, B.; Limberg, C.; Herwig, C.; Mebs, S. *Angew. Chem., Int. Ed.* **2011**, *50*, 12621.
- (9) Page, M. J.; Lu, W. Y.; Poulten, R. C.; Carter, E.; Algarra, A. G.; Kariuki, B. M.; Macgregor, S. A.; Mahon, M. F.; Cavell, K. J.; Murphy, D. M.; Whittlesey, M. K. *Chem.—Eur. J.* **2013**, *19*, 2158.
- (10) The oxidation of a five-membered IMes ligand (IMes = 1,3-bis(2,4,6-trimethylphenyl)imidazol-2-ylidene) by N₂O has recently been reported in a dinuclear Ru–NHC complex. Tskhovrebov, A. G.; Solari, E.; Scopelliti, R.; Severin, K. *Organometallics* **2012**, *31*, 7235.
- (11) Hudnall, T. W.; Moerdyk, J. P.; Bielawski, C. W. *Chem. Commun.* **2010**, 46, 4288.
- (12) Wiggins, K. M.; Moerdyk, J. P.; Bielawski, C. W. *Chem. Sci.* **2012**, *3*, 2986.
- (13) Sheldrick, G. M. *Acta Crystallogr.* **1990**, A467–473, 46. Sheldrick, G. M., SHELXL-97, a computer program for crystal structure refinement, University of Göttingen, 1997.

(14) (a) Gunay, A.; Theopold, K. H. *Chem. Rev.* **2010**, *110*, 1060. (b) Garcia-Bosch, I.; Ribas, X.; Costas, M. *Eur. J. Inorg. Chem.* **2012**, 179.

(15) For C–H bond oxidation reactions of other ligands at Ni, see: (a) Itoh, S.; Bandoh, H.; Nagatomo, S.; Kitagawa, T.; Fukuzumi, S. *J. Am. Chem. Soc.* **1999**, *121*, 8945. (b) Hikichi, S.; Yoshizawa, M.; Sasakura, Y.; Komatsuzaki, H.; Moro-oka, Y.; Akita, M. *Chem.—Eur. J.* **2001**, *7*, 5012. (c) Cho, J.; Furutachi, H.; Fujinami, S.; Suzuki, M. *Angew. Chem., Int. Ed.* **2004**, *43*, 3300. (d) Cho, J.; Furutachi, H.; Fujinami, S.; Tosha, T.; Ohtsu, H.; Ikeda, O.; Suzuki, A.; Nomura, A.; Uruga, T.; Tanida, H.; Kawai, T.; Tanaka, K.; Kitagawa, T.; Suzuki, M. *Inorg. Chem.* **2006**, *45*, 2873. (e) Yao, S. L.; Herwig, C.; Xiong, Y.; Company, A.; Bill, E.; Limberg, C.; Driess, M. *Angew. Chem., Int. Ed.* **2010**, *49*, 7054.

(16) Kunishita, A.; Doi, Y.; Kubo, M.; Ogura, T.; Sugimoto, H.; Itoh, S. *Inorg. Chem.* **2009**, *48*, 4997.

(17) IPr = 1,3-bis(2,6-diisopropylphenyl)imidazol-2-ylidene.

(18) Dible, B. R.; Sigman, M. S. *J. Am. Chem. Soc.* **2003**, *125*, 872.

(19) (a) Carmona, E.; Marín, J. M.; Paneque, M.; Poveda, M. L. *Organometallics* **1987**, *6*, 1757. (b) Vanderlende, D. D.; Abboud, K. A.; Boncella, J. M. *Inorg. Chem.* **1995**, *34*, 5319. (c) Cámpora, J.; Palma, P.; del Río, D.; Álvarez, E. *Organometallics* **2004**, *23*, 1652.

(20) A related complex has very recently been prepared by Braunstein and co-workers through the double deprotonation of an alcohol functionalized imidazolium salt in the presence of Ni(dme)Cl₂. Hameury, S.; de Frémont, P.; Breuil, P.-A. R.; Olivier-Bourbigou, H.; Braunstein, P. *Inorg. Chem.* **2014**, *53*, 5189.

(21) Unfortunately, we have been unable to find a synthetic route to **6** to allow full structural characterization.

(22) (a) César, V.; Lugan, N.; Lavigne, G. *J. Am. Chem. Soc.* **2008**, *130*, 11286. (b) Hudnall, T. W.; Bielawski, C. W. *J. Am. Chem. Soc.* **2009**, *131*, 16039. (c) César, V.; Lugan, N.; Lavigne, G. *Eur. J. Inorg. Chem.* **2010**, 361. (d) Moerdyk, J. P.; Bielawski, C. W. *Organometallics* **2011**, *30*, 2278. (e) Blake, G. A.; Moerdyk, J. P.; Bielawski, C. W. *Organometallics* **2012**, *31*, 3373. (f) Moerdyk, J. P.; Bielawski, C. W. *Chem.—Eur. J.* **2013**, *19*, 14773.

(23) (a) Cotton, F. A.; Goodgame, D. M. L. *J. Am. Chem. Soc.* **1960**, *82*, 5771. (b) Daniels, W. E. *Inorg. Chem.* **1964**, *3*, 1800.

(24) This route also afforded the corresponding pyrimidinium salts of [Ni(PPh₃)Br₃][−] in significant amounts. See Supporting Information for characterization. See also: Xu, Y. C.; Zhang, J.; Sun, H. M.; Shen, Q.; Zhang, Y. *Dalton Trans.* **2013**, *42*, 8437.

(25) Matsubara, K.; Ueno, K.; Shibata, Y. *Organometallics* **2006**, *25*, 3422.

(26) Iglesias, M.; Beetstra, D. J.; Kariuki, B.; Cavell, K. J.; Dervisi, A.; Fallis, I. A. *Eur. J. Inorg. Chem.* **2009**, 1913.